GBT Prime Focus (Band 1-4): All Sky Pointing at 800 MHz

Dana S. Balser, Ronald J. Maddalena, Frank Ghigo, & Glen I. Langston

14 September 2001

Abstract

All sky pointing observations at Prime Focus (Band 1-4) are discussed. A traditional pointing model including eight physical terms are used to fit the data. The all sky *rms* is 15.″2.

1 Introduction

The first all sky pointing observations at Prime Focus were made using Band 1-4 at a sky frequency of 800 MHz. Focus tracking was employed for the X and Y directions using an empirically determined algorithm. The observations and analysis are discussed in §2. AIPS++ was used to reduce the pointing data while the program TPOINT determined the pointing model. The results and conclusions are in §3 and §4, respectively.

2 Observations and Analysis

Observations were taken during two epochs: 2001 August 19 (project pnt_prime_20) and 2001 August 23 (project pnt_prime_21). All pointing sources were selected from the NVSS pointing calibrator list (Condon & Yin 2001, PASP, 113, 362). The GBT half-power beam-width (HPBW) is $\sim 15'$ at 800 MHz. The observing file "allsky_pf.obs" was created with the CLEO application *scheduler* using slew rates of 10° per minute in azimuth with an acceleration time of 0.2 minutes, and 7.°9 per minute in elevation with an acceleration time of 0.09 minutes.[1] A procedure time of 2.7 min was estimated for each pointing which includes overhead time.

The telescope focus and pointing are coupled. Therefore the focus was determined first and then implemented during the all sky pointing observations. The prime focus system has three

[1]The maximum Az rate was lowered to 10° per minute (quarter speed) because of high accelerations measured during hard stops. Currently new brakes are on order.

degrees of freedom: an axial motion (Y), a lateral motion along the line of symmetry (X), and a rotation (POLAR). The focus tracking for the X and Y directions has been determined using astronomical observations (Balser et al. 2001, GBT Com. Memo 12). Both X and Y were determined as a function of elevation (E) at a frequency of 800 MHz where

$$\mathrm{X} = 780.8 - 329.4\,\mathrm{Cos(E)} - 84.5\,\mathrm{Sin(E)}\ \ \mathrm{mm} \tag{1}$$

and

$$\mathrm{Y} = 1203 - 263.7\,\mathrm{Cos(E)} + 84.5\,\mathrm{Sin(E)}\ \ \mathrm{mm}. \tag{2}$$

The pnt_prime_20 observing session occurred over a weekend. Many problems with both the hardware and software caused much of the first observing period to be compromised. Only the second day's worth of data were used in the current analysis. The pnt_prime_21 observing period consisted of one evening during the week. Only 50% of these data were acceptable because of interference and some problems with software which made it difficult to recover all the necessary antenna information.

The GO procedure *peak* was used to determine local pointing corrections (LPCs). The procedure *peak* performs two raster scans in RA ($W \rightarrow E$ and then $E \rightarrow W$). The procedure then pauses. An event is sent to an AIPS++ client which fills the data using *gbtmsfiller*, and then calculates the LPCs. If acceptable the LPCs are updated automatically and then the procedure performs two raster scans in Dec ($S \rightarrow N$ and then $N \rightarrow S$). Again the data are filled, analyzed, and the LPCs updated pending user verification. A telescope rate of $150'$ per minute was used with a length of $75'$ and an integration time of 0.1 s.

The data were analyzed using the AIPS++ DCR tool offline. The procedure *Point1* performs a first-order polynomial baseline fit using the first and last 10% of the scan, subtracts this model from the data, and then fits a Gaussian model to the resulting profile. The observed source position $(A_{\mathrm{obs}}, E_{\mathrm{obs}})$ is determined from the center position of the Gaussian model profile. The NVSS source J2000 equatorial coordinates are converted into horizon coordinates at the midpoint of the scan and are denoted as (A_*, E_*). The local pointing offset is just the difference between these two coordinates. Therefore,

$$\Delta A = A_{\mathrm{obs}} - A_* \tag{3}$$

and

$$\Delta E = E_{\mathrm{obs}} - E_*. \tag{4}$$

The new LPCs are just the old values plus the local pointing offset determined in Equations (3) and (4).

The indicated telescope position is the difference between the know source position and the measured position. Therefore the LPCs which were used in the pointing measurement along

Table 1: Azimuth Pointing Terms (ΔA Cos E)

Coeff. (M&C)	Coeff. (TPOINT)	Term	Value (arcsec)	σ (arcsec)	Meaning
$d_{0,0}$	–CA	1	–58.67	26.370	Horizontal Collimation
$b_{0,1}$	–NPAE	Sin E	+65.27	17.288	El Axle Collimation
$d_{0,1}$	–IA	Cos E	–81.14	21.957	Az Zero
$b_{1,1}$	AW	Cos A Sin E	+2.97	1.557	Zenith E-Tilt
$a_{1,1}$	AN	Sin A Sin E	+3.70	1.579	Zenith N-Tilt

with the contribution from the traditional pointing model have to be included. So

$$A_{\rm tel} = A_* - (A_{\rm tm} + A1_{\rm lpc}\,{\rm Cos(E)} + A2_{\rm lpc} + \Delta A)/{\rm Cos(E)} \tag{5}$$

and

$$E_{\rm tel} = E_* - (E_{\rm tm} + E_{\rm lpc} + \Delta E) \tag{6}$$

where ($A_{\rm tm}$, $E_{\rm tm}$) are the contributions from the traditional pointing model and ($A1_{\rm lpc}$, $A2_{\rm lpc}$, $E_{\rm lpc}$) are the local pointing corrections.

3 Results

The all sky pointing observations are summarized in Figures 1–2. There are 117 and 31 points corresponding to pnt_prime_20 (Figure 1) and pnt_prime_21 (Figure 2), respectively. The program TPOINT was used to perform a multi-dimensional least-squares fit to the data (Wallace 1998). Both observing runs (pnt_prime_20) and (pnt_prime_21) were combined for this analysis. A traditional model which includes eight physical terms was used. The pointing coefficients are listed in Tables 1 and 2 for the azimuth and elevation series, respectively.

The sky root-mean-square (rms) of the fit is 15.″2. This is a factor of 1.8 higher than the rms of 8.″5 determined at S-band. The accuracy of a pointing measurement is given by Nguyen-Quang-Rieu (1969, A&A, 1, 128) where the uncertainty in right ascension is given by

$$\Delta t_{\rm rms} = 0.5\sqrt{\theta_{\rm obs}\theta_{\rm b}/{\rm Cos}\delta}\,(N/S), \tag{7}$$

where $\theta_{\rm obs}$ is the observed linewidth, $\theta_{\rm b}$ is the telescope HPBW, δ is the declination, and (S/N) is the signal-to-noise ratio. Therefore, for a point source the uncertainty goes as $\theta_{\rm b}/$ (S/N). The PF HPBW at 800 MHz is 2.5 times larger than at S-band. Since many of the

Table 2: Elevation Pointing Terms (ΔE)

Coeff. (M&C)	Coeff. (TPOINT)	Term	Value (arcsec)	σ (arcsec)	Meaning
$d_{0,0}$	IE	1	−563.02	26.320	El Zero
$c_{1,0}$	−AW	Sin A	−2.97	1.557	Zenith E-Tilt
$d_{1,0}$	AN	Cos A	+3.70	1.579	Zenith N-Tilt
$b_{0,1}$	ECES	Sin E	+703.61	17.226	Asymmetric Gravity
$d_{0,1}$	ECEC	Cos E	+518.29	21.875	Symmetric Gravity

pointing sources are extragalactic where $F_\nu \propto \nu^{-0.7}$, the S/N ratio of the PF data should be higher than the S-band data by almost a factor of 2 on average. Therefore, the uncertainty of the PF 800 MHz data should be greater than the S-band data by a factor of 1.3. This is less than observed, although the RFI was significantly worse at the lower frequencies which will lower the effective S/N ratio and increase the uncertainty of the pointing residuals.

The determined pointing coefficients at PF are different than those determined at S-band (see Balser et al. 2001, GBT Com. Memo 6).[2] Because many of the terms are correlated this is not unexpected. In both pointing runs the focus tracking in the Z direction was not employed. At Gregorian focus the full range of motion in the Z direction did not produce sufficient gain variations while at PF there is no means to move in Z. These show up as pointing errors in the first three terms of the azimuth series. The gravity terms in the elevation series are similar but smaller for the PF data. In both prime and Gregorian focus the zenith tilt terms are small.

The correlations in the fit are shown below. They are similar to that obtained at S-band. The gravity coefficients along with the El zero are highly correlated. The first three azimuth terms, expected to fit the Z focus tracking motion, are highly correlated.

```
IE      -0.0012
NPAE    +0.9471 -0.0017
CA      -0.9924 +0.0014 -0.9763
AW      -0.0555 -0.0288 -0.0356 +0.0452
AN      +0.0103 -0.0044 +0.0136 -0.0104 -0.0213
ECEC    +0.0018 -0.9919 +0.0024 -0.0021 +0.0271 +0.0358
ECES    -0.0005 -0.9756 +0.0000 +0.0002 +0.0348 -0.0236 +0.9448

          IA      IE      NPAE    CA      AW      AN      ECEC
```

[2]Notice that the signs for all of the coefficients are reversed because of a sign error in the S-band analysis. This was revealed when the pointing model was first applied.

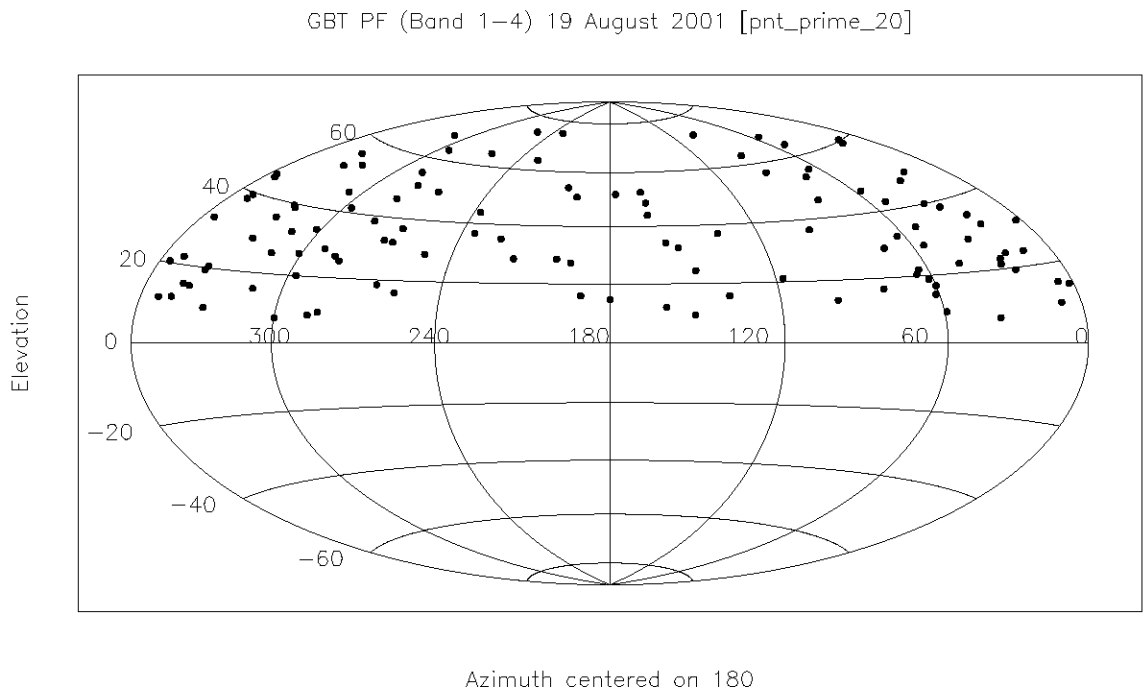

Figure 1: Distribution of sources on the sky with an aitoff projection for project pnt_prime_20.

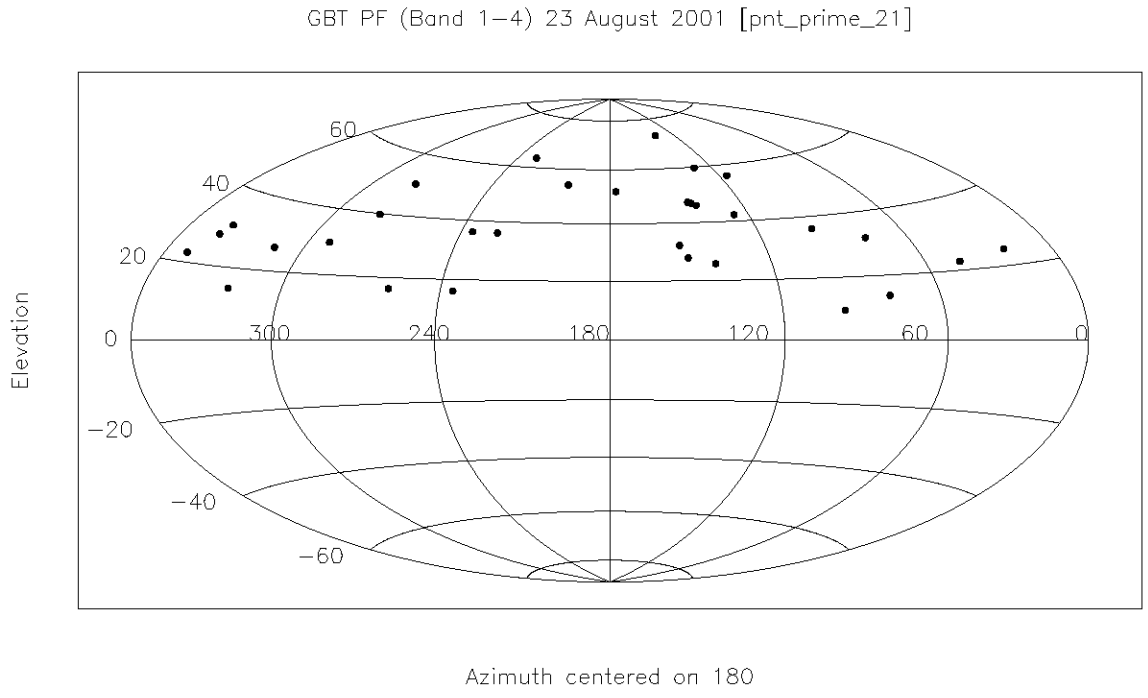

Figure 2: Distribution of sources on the sky with an aitoff projection for project pnt_prime_21.

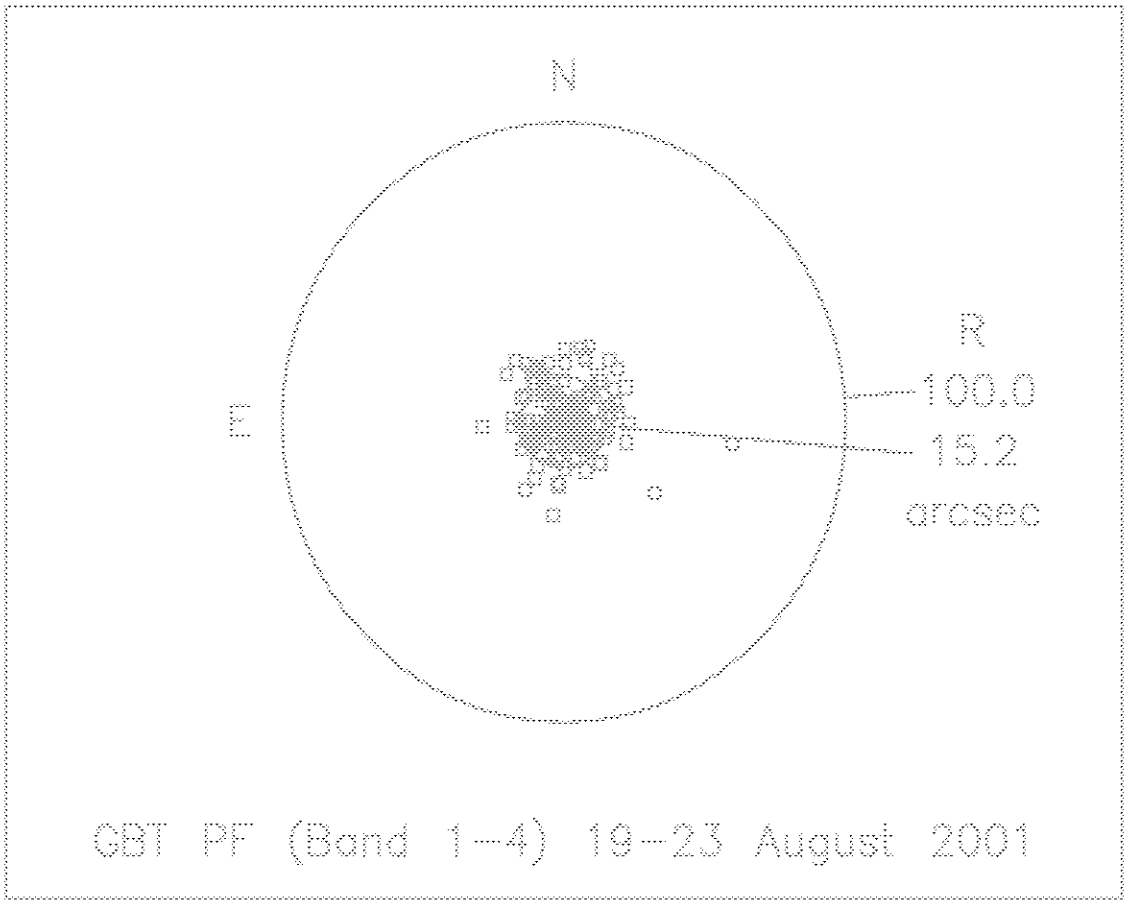

Figure 3: The residuals plotted as a scatter diagram. The inner circle is the sky *rms* of the fit (15.″2).

Various plots of the residuals to the fit are shown in Figures 3–8. There appears to be nonrandom structure in some of these plots. For example, there appears to be sinusoidal features in the pointing error in zenith angle versus azimuth.

4 Conclusions

All sky pointing observations were made during two distinct periods within a week of each other. Because of technical difficulties and RFI only a total of 148 measurements were made. A traditional pointing model consisting of eight physical terms produces a sky *rms* of 15.″2. Many of the pointing terms determined at prime focus are different in detail from the S-band data taken at Gregorian focus. In both cases the zenith tilt of the azimuth track is small ($\lesssim$ few arcsec) while the gravity terms are large ($\gtrsim 10'$).

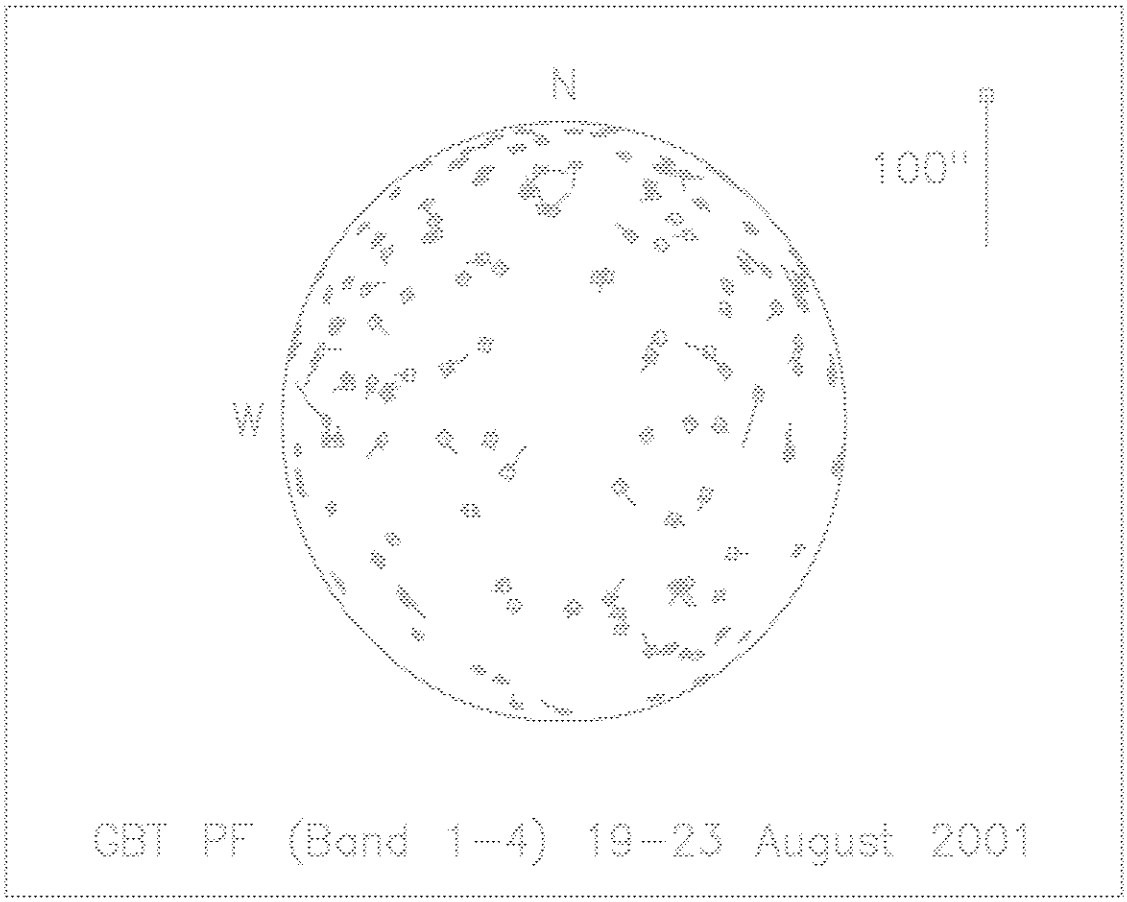

Figure 4: The pointing residuals as error vectors on an azimuthal projection.

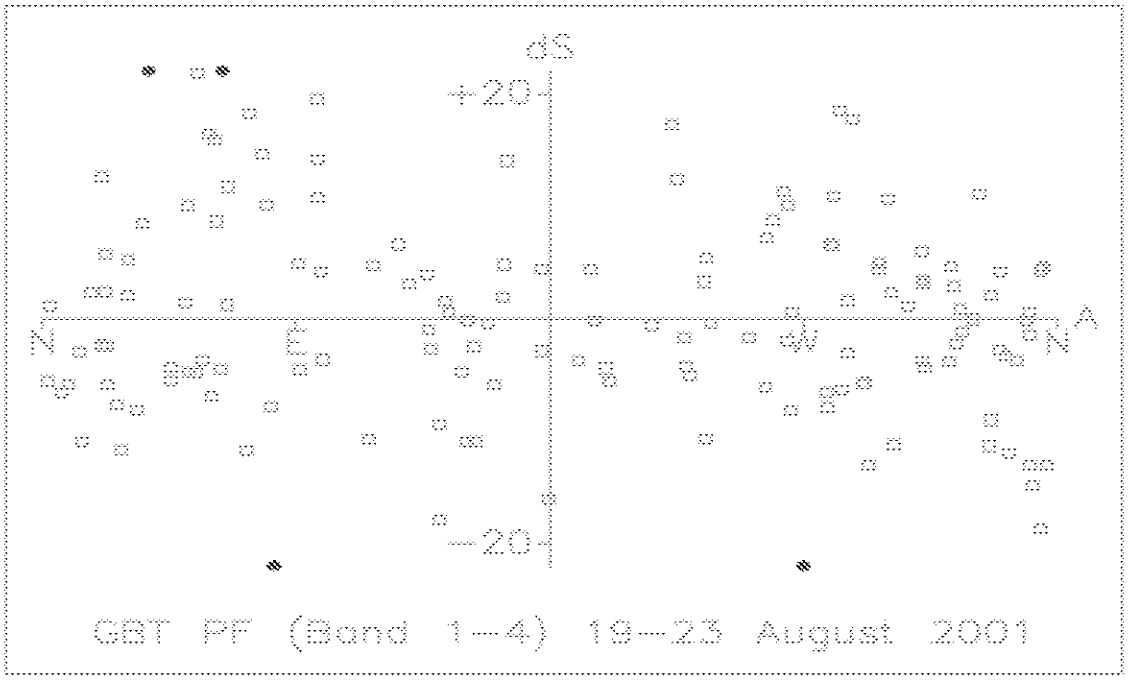

Figure 5: The pointing error horizontally on the sky (ΔA Cos E) as a function of azimuth.

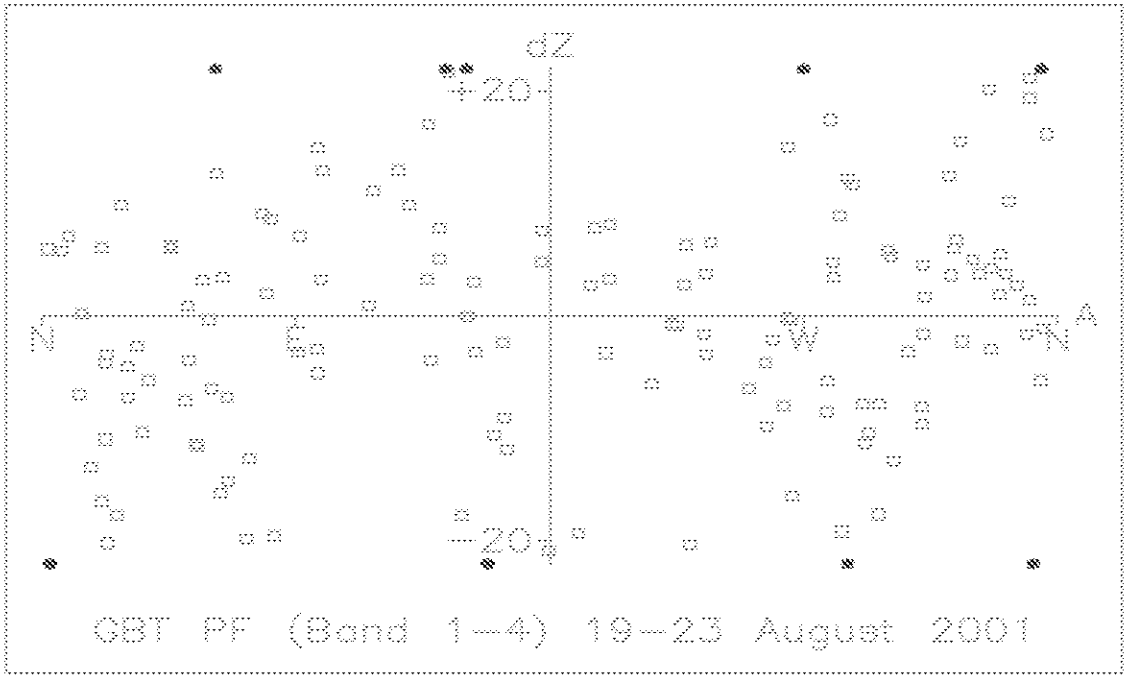

Figure 6: The pointing error in zenith angle as a function of azimuth.

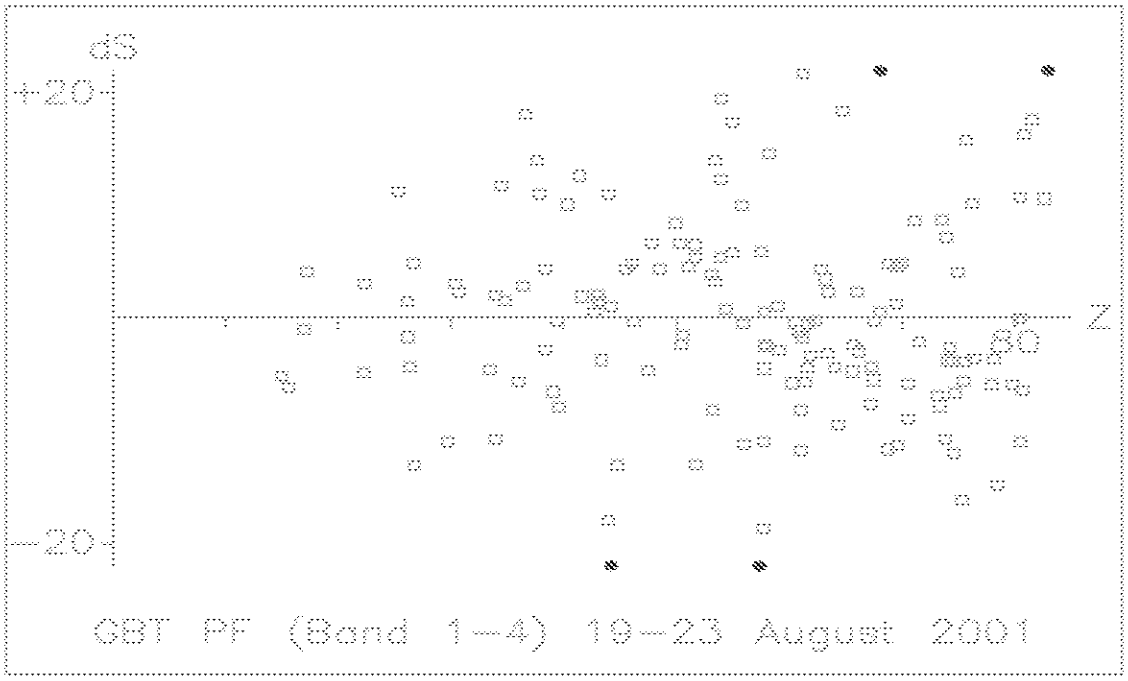

Figure 7: The pointing error horizontally on the sky (ΔA Cos E) as a function of zenith angle.

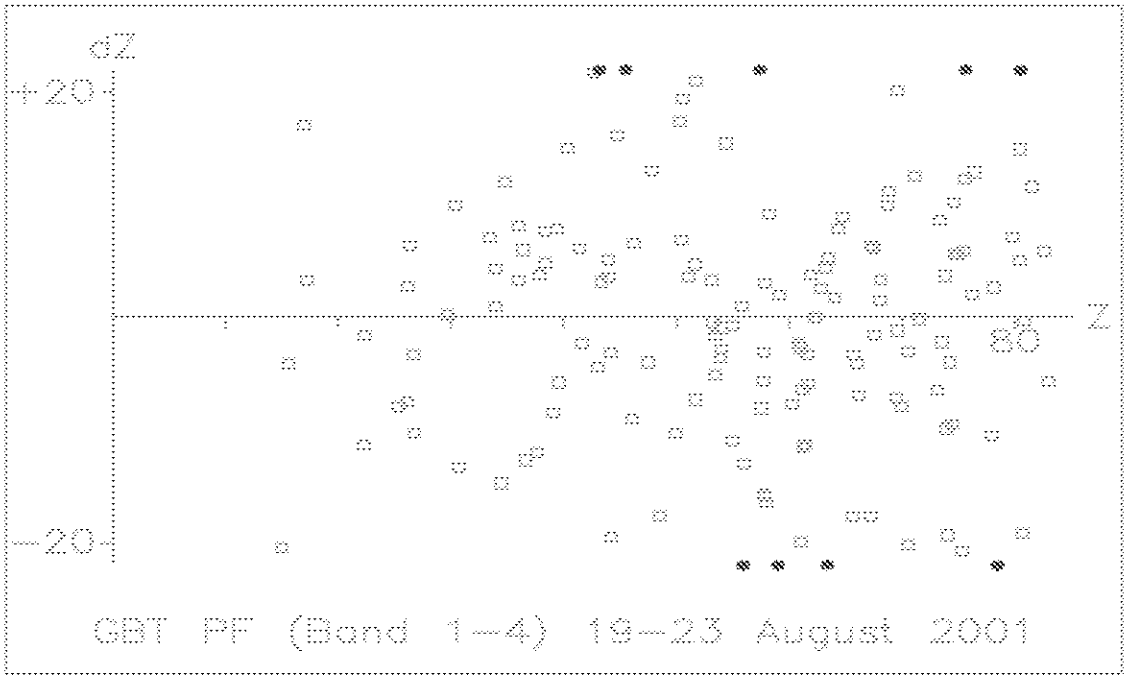

Figure 8: The pointing error in zenith angle as a function of zenith angle.